[Imaging]

Magnetic Resonance Imaging of the Elbow: A Structured Approach

Srinath C. Sampath, MD, PhD,† Srihari C. Sampath, MD, PhD,† and Miriam A. Bredella, MD*†

Context: The elbow is a complex joint and commonly injured in athletes. Evaluation of the elbow by magnetic resonance imaging (MRI) is an important adjunct to the physical examination. To facilitate accurate diagnosis, a concise structured approach to evaluation of the elbow by MRI is presented.

Evidence Acquisition: A PubMed search was performed using the terms *elbow* and *MR imaging*. No limits were set on the range of years searched. Articles were reviewed for relevance with an emphasis of the MRI appearance of normal anatomy and common pathology of the elbow.

Results: The spectrum of common elbow disorders varies from obvious acute fractures to chronic overuse injuries whose imaging manifestations can be subtle. MRI evaluation should include bones; lateral, medial, anterior, and posterior muscle groups; the ulnar and radial collateral ligaments; as well as nerves, synovium, and bursae. Special attention should be paid to the valgus extension overload syndrome and the MRI appearance of associated injuries when evaluating throwing athletes.

Conclusion: MRI evaluation of the elbow should follow a structured approach to facilitate thoroughness, accuracy, and speed. Such an approach should cover bone, cartilage, muscle, tendons, ligaments, synovium, bursae, and nerves.

Keywords: elbow; magnetic resonance imaging; tendons; ligaments

Elbow pain is a common complaint among competitive and recreational athletes, as well as those subject to chronic repetitive occupational injuries. Evaluation of the elbow by magnetic resonance imaging (MRI) is an important adjunct to the physical examination and can provide information not easily obtainable even at surgery. To maximize the diagnostic yield of MRI, a structured approach is critical. Here, we provide such a diagnostic algorithm, beginning with a discussion of protocols, followed by a review of the relevant normal anatomy and common elbow pathology and, finally, a structured approach to reviewing elbow MRI examinations.

PROTOCOL

Evaluation of the elbow on MRI begins with proper patient positioning, which should maximize comfort and thereby minimize motion. This is usually accomplished with the patient in supine position and the arm held at the side in anatomical position (ie, supinated). A disadvantage of this position is the location of the arm away from the isocenter of the magnet, which degrades signal-to-noise and field homogeneity and, therefore, image quality. For this reason, some radiologists advocate prone positioning with the arm over the head ("Superman position"). In either case, the highest-quality images are obtained using dedicated surface coils.

The field of view should cover the distal humeral metaphysis to the bicipital tuberosity of the radius. The latter is particularly crucial in known or suspected cases of biceps tendon injury/rupture. Imaging should be performed in all 3 planes, as certain structures are best seen in different planes (ie, nerves in the axial plane, ligaments in the coronal, and biceps tendon in the sagittal plane). The choice of sequences varies by institution but should include both non-fat-saturated T1-weighted and proton density–weighted sequences as well as fat-saturated T2/proton density–weighted or short tau inversion recovery sequences, which are critical for evaluation of potential bony injury. Gradient echo sequences are not routinely necessary but can be added if there is specific clinical suspicion for loose bodies or synovial abnormality, such as pigmented villonodular synovitis or hemophilia (discussed in the following).

From † Massachusetts General Hospital and Harvard Medical School, Boston, Massachusetts
*Address correspondence to Miriam A. Bredella, MD, Associate Professor of Radiology, Harvard Medical School, Department of Radiology, Massachusetts General Hospital, Yawkey 6E, 55 Fruit Street, Boston, MA 02114 (e-mail: mbredella@partners.org).
The authors report no potential conflicts of interest in the development and publication of this manuscript.
DOI: 10.1177/1941738112467941

Table 1. Elbow magnetic resonance imaging protocol at 1.5 T.

Sequence	FOV, mm	Slice Thickness, mm	TR, ms	TE, ms	TI, ms	NEX	Bandwidth, kHz
PD TSE Ax	140 × 100	4	2500	30		2	203
T2 TSE FS Ax	140 × 100	4	3000	53		2	211
T1 TSE Cor	140 × 100	3	641	10		1	199
T2 TSE FS Cor	140 × 100	4	3060	50		2	150
T2 GRE Cor	140 × 100	3	467	19		1	105
PD TSE FS Sag	140 × 100	4	1710	34		1	180
STIR Cor (optional)	160 × 100	4	4810	29	160	1	130
T1 FS Cor (optional)	140 × 100	3	586	10		1	199
T1 FS Ax (optional)	140 × 100	1	586	10		1	199
T1 FS Sag (optional)	140 × 100	3	586	10		1	199

FOV, field of view; TR, repetition time; TE, echo time; TI, inversion time; NEX, number of excitations; PD, proton density; TSE, turbo spin echo; Ax, axial; FS, fat saturation; Cor, coronal; GRE, gradient echo; STIR, short tau inversion recovery; Sag, sagittal.

Table 2. Elbow magnetic resonance arthrogram protocol at 1.5 T.

Sequence	FOV, mm	Slice Thickness, mm	TR, ms	TE, ms	NEX	Bandwidth, kHz
T1 TSE Cor	140 × 100	3	525	14	1	130
T1 TSE FS Cor	140 × 100	3	500	13	1	130
T2 TSE FS Cor	140 × 100	3	3000	46	1	200
T2 TSE FS Ax	140 × 100	3	3880	46	1	200
T2 TSE FS Sag	140 × 100	3	3880	46	1	200
PD TSE Ax	140 × 100	3	2500	33	2	159

FOV, field of view; TR, repetition time; TE, echo time; NEX, number of excitations; TSE, turbo spin echo; Cor, coronal; FS, fat saturation; Ax, axial; Sag, sagittal; PD, proton density.

Similarly, the routine administration of gadolinium-based contrast material—either intravenous or intra-articular—is not considered necessary. Intravenous contrast can be given if there is concern for mass, synovitis, or inflammatory arthropathy. Intra-articular contrast in turn is particularly useful for outlining ligament tears or assessing the stability of known or suspected loose bodies. In such cases, approximately 5 to 10 mL of routine dilute gadolinium (1:250) is injected with a 25- or 22-gauge needle via any standard approach. Both fat-saturated and non-fat-saturated T1- and proton density/T2-weighted or short tau inversion recovery sequences should be obtained.[9,22,46]

For reference, the authors' institutional protocol for routine elbow MRI as well as magnetic resonance arthrography (MRA) is given in Tables 1 and 2.

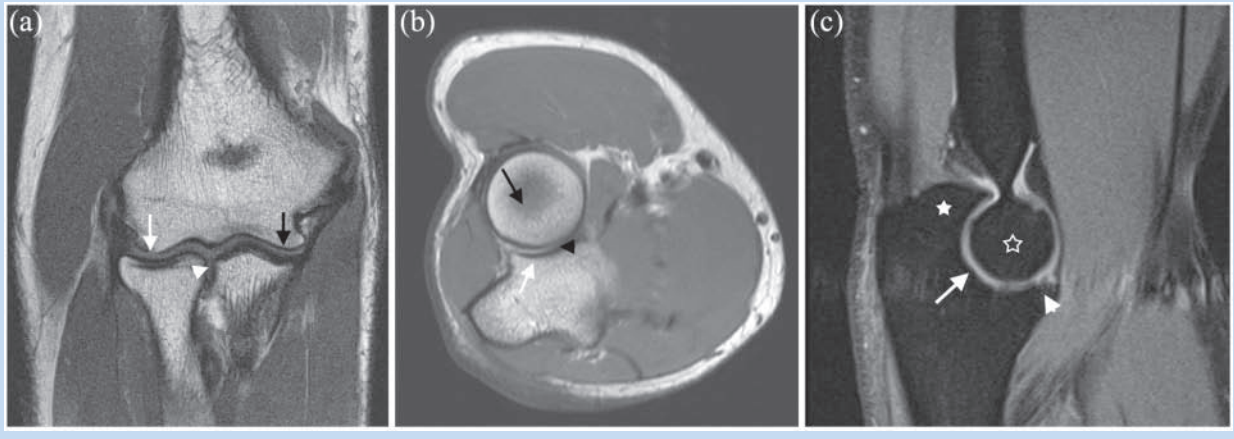

Figure 1. Normal osseous anatomy of the elbow. (a) Coronal T1-weighted image demonstrates the ulnohumeral joint (black arrow), the radiocapitellar joint (white arrow), and the radioulnar joint (arrowhead). (b) Axial proton density–weighted image demonstrates the radioulnar articulation (arrowhead) between the radial head (black arrow) and the radial notch of the ulna (white arrow). (c) Sagittal fat-saturated T2-weighted image demonstrates normal ulnohumeral articulation between the ulnar trochlear notch (white arrow) and the trochlea (open star). Note the olecranon (solid star) and coronoid process (arrowhead) of the ulna.

NORMAL ANATOMY

The elbow is a complex joint comprising the articulations among 3 bones: the humerus, radius, and ulna (Figure 1). These articulations allow a combination of flexion, extension, pronation, and supination of the forearm.[1,22,26,31]

The joint capsule of the elbow is thickened medially and laterally to form the respective collateral ligament complexes. The ulnar collateral ligament complex extends from the medial epicondyle of the humerus to the sublime tubercle of the medial coronoid process of the ulna and is the most important medial stabilizer of the elbow joint. The ulnar collateral ligament (Figure 2) comprises 3 bands: the anterior band, which provides significant restraint to valgus stress; the posterior band; and the functionally less significant transverse band. The radial collateral ligament complex (Figure 3) provides varus stability and comprises 4 parts: the annular ligament, which courses around the radial head and attaches to the sigmoid notch of the ulna; the radial collateral ligament, which extends from the lateral epicondyle to the annular ligament; the lateral ulnar collateral ligament (LUCL), which runs more posteriorly from the lateral epicondyle to the supinator crest of the ulna; and the accessory collateral ligament, which is variably present.[1,22,26,30,41]

Four muscle compartments (medial, lateral, anterior, and posterior) are found about the elbow. Of these, the medial and lateral muscle compartments are particularly important when evaluating elbow injuries, as their respective common tendons lie in proximity to the related collateral ligaments. These muscles originate from the medial epicondyle by way of the common flexor tendon (Figure 4a) and from the lateral epicondyle by way of the common extensor tendon (Figure 4b).

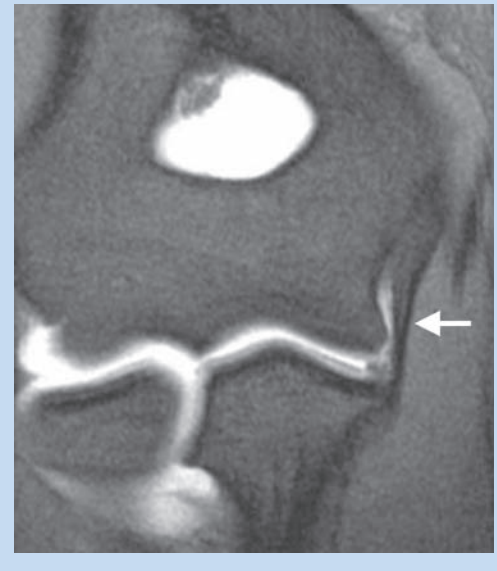

Figure 2. Coronal fat-saturated T1-weighted image from a magnetic resonance arthrogram demonstrates the normal anterior band of the ulnar collateral ligament (arrow) extending from the inferior aspect of the medial epicondyle to the sublime tubercle of the coronoid process of the ulna.

The common flexor tendon comprises the tendons of the medial group muscles, the pronator teres, flexor carpi radialis, flexor carpi ulnaris, flexor digitorum superficialis, and palmaris longus and inserts on the medial epicondyle just proximal to the ulnar collateral ligament. Likewise, the common extensor

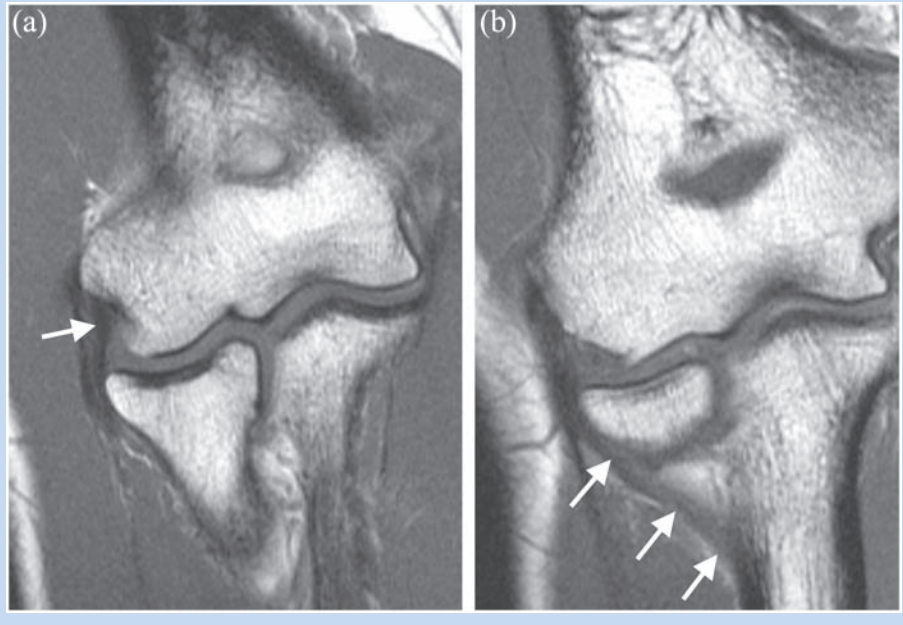

Figure 3. Normal anatomy of the radial collateral ligament complex. (a) Coronal T1-weighted image demonstrates the origin of the radial collateral ligament and lateral ulnar collateral ligament (LUCL) on the lateral epicondyle (arrow). (b) The LUCL courses posteromedially from the lateral epicondyle to the supinator crest of the ulna (arrows).

tendon comprises the tendons of the lateral group muscles, the brachioradialis, extensor carpi radialis longus and brevis, extensor digitorum, extensor carpi ulnaris, and the supinator and inserts on the lateral epicondyle. The anterior muscle compartment includes the biceps brachii and brachialis (Figures 4c and 4d); the former inserts distally on the radial tuberosity of the radius while the posterior group comprises the triceps tendon (Figure 4e) and anconeus and, in some cases, the anconeus epitrochlearis (Figure 4f).[1,17,22,26,41]

The neurovascular structures of the elbow, which are well visualized on MRI, include the ulnar nerve, which takes a superficial course along the posteromedial humerus and lies within the cubital tunnel (Figure 5); the median nerve, which runs in a superficial course posterior to the bicipital aponeurosis (lacertus fibrosus) and anterior to the brachialis muscle; the radial nerve, which is found anterior to the lateral epicondyle, between the brachialis and brachioradialis muscles; and the brachial artery, which runs medial to the biceps tendon in the antecubital fossa.[22,26]

APPROACH

MRI evaluation of the elbow should follow a structured approach to facilitate thoroughness, accuracy, and speed. Such an approach should cover all the major categories discussed in the Anatomy section (ie, bone/marrow/cartilage, muscle, tendons, ligaments, and nerves). The exact order of evaluation is less important than reproducibility in approach and completeness in examining all visualized structures.

Bone

Our approach begins with evaluation of bones and bone marrow. As most cases of suspected injury to the elbow are first evaluated by plain radiography, this approach has the advantage of beginning with correlation to any abnormalities noted on radiographs. In case of acute traumatic injury, evaluation should begin with assessment of alignment at the 3 joints of the elbow: the radiocapitellar, ulnohumeral, and radioulnar articulations. The elbow is usually imaged in supine position with the arm at the side (supination), and dynamic instability, in the case of ligamentous injury, can be missed.[8]

After proper alignment is confirmed, displaced or nondisplaced fractures are evaluated on T1 and fat-saturated proton density/T2-weighted images. While most fractures should be evident as hypointense lines on T1-weighted images, it is critical to carefully scrutinize fat-saturated T2-weighted images for areas of stress reaction or bone marrow edema/contusion, which may be missed on T1-weighted images. MRI is the modality of choice for the detection of radiographically occult fractures, particularly of the radial head, which are often suspected on the basis of persistent pain or joint effusion (Figure 6).[7] Bone marrow edema can also help to define mechanisms and discrete patterns of injury, which are encountered in both recreational and elite athletes. For instance, both medial epicondylitis (golfer's elbow) and lateral epicondylitis (tennis elbow) can be seen in association with bone marrow edema. In such cases, bone marrow edema can provide a clue for closer scrutiny of tendon or ligamentous injury.

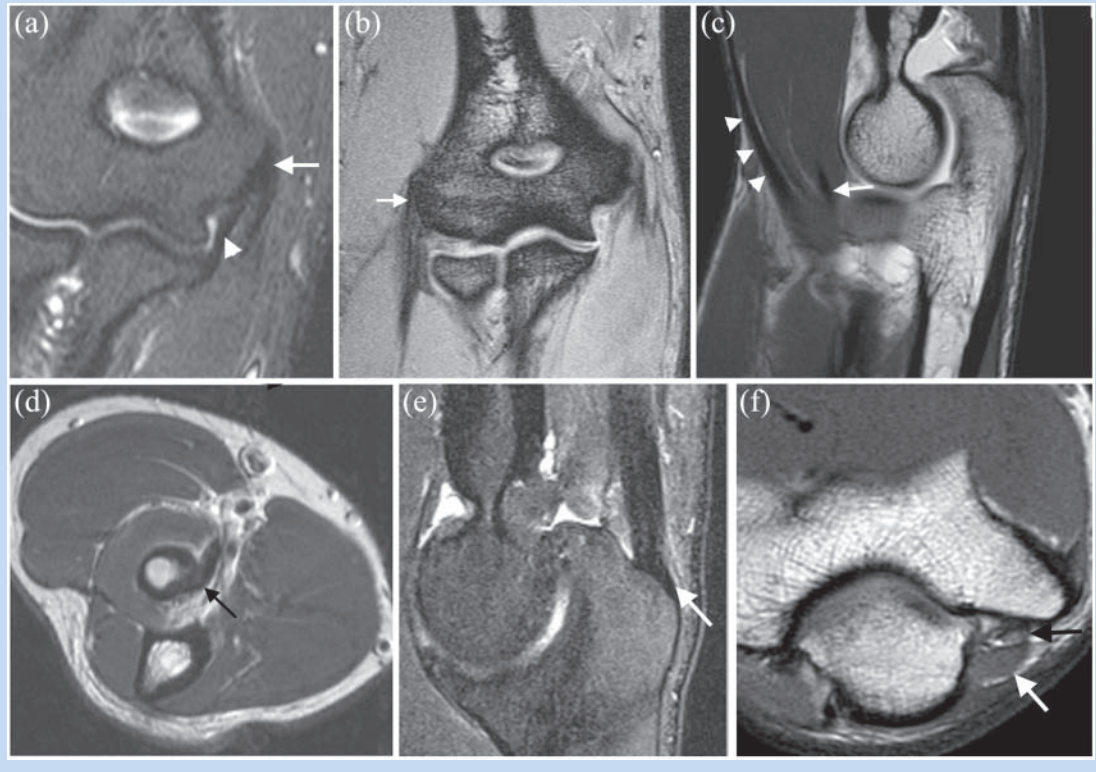

Figure 4. Normal anatomy of elbow muscle compartments. (a) Coronal fat-saturated proton density–weighted image demonstrates normal low signal intensity of the common flexor tendon at the medial epicondyle (arrow). Note the normal ulnar collateral ligament (arrowhead). (b) Coronal gradient echo image demonstrates normal appearance of the common extensor tendon at the lateral epicondyle (arrow). (c) Sagittal T1-weighted image from a magnetic resonance arthrogram demonstrates normal tendon of biceps (arrowheads) and brachialis (arrow) in the anterior compartment. (d) Axial proton density–weighted image demonstrates normal biceps tendon insertion onto the radial tuberosity (arrow). It is important to always include the radial tuberosity on the axial images. (e) Sagittal fat-saturated T2-weighted image demonstrates normal triceps tendon insertion onto the olecranon (arrow). (f) Axial proton density–weighted image demonstrates anconeus epitrochlearis (white arrow), an accessory muscle of the posterior compartment. Note the proximity to the ulnar nerve (black arrow), which can be compressed by the muscle, leading to cubital tunnel syndrome.

Two common forms of bone injury are osteochondrosis and osteochondritis dissecans or osteochondral defect (OCD). Osteochondrosis represents a developmental form of avascular necrosis that most often involves the capitellum (Panner disease). This usually affects boys from 7 to 12 years of age, preceding complete ossification of the capitellar ossification center.[24] On MRI, Panner disease manifests as abnormal T2 hyperintensity and T1 hypointensity in a geographic region of the capitellum (Figure 7). Although it progresses to sclerosis and fragmentation (readily appreciated on radiographs), the prognosis is usually good.[25,27] OCD, by contrast, is an acquired focal lesion of bone and cartilage, most often affecting the capitellum, and felt to be related to repetitive valgus stress as seen in young competitive athletes. It typically affects older children (12-16 years) and is recognized on MRI as an intermediate to low T1 signal subchondral lesion with or without demonstrable overlying cartilage injury (Figure 8).[40] As with osteochondral injury elsewhere (eg, in the knee), displacement or fluid undercutting the fragment is indicative of instability and may represent an indication for intervention.[11]

A common misdiagnosis is the pseudodefect of the capitellum. This is a partial volume effect caused by sharp angulation of the posterior margin of the capitellum, which can cause a focal-appearing "pseudolesion" on sagittal or coronal images (Figure 9). Examination in other planes or with MRA will often clarify the nature of the finding, as will recognition of the posterior location of the pseudodefect, whereas most OCDs occur anteriorly.[37,42]

Unstable OCD, osteoarthritis, or fractures can result in intra-articular loose bodies, the evaluation for which is an important indication for MRI. While MRA is helpful for outlining loose osteochondral bodies, conventional MRI is sufficient, particularly if a joint effusion is present. Loose bodies tend to collect in the olecranon and coronoid fossae and, when large, can appear hyperintense on T1-weighted images due to fatty marrow. They are otherwise identified as hypointense filling defects in hyperintense joint effusion on T2-weighted images or within hyperintense intra-articular contrast on fat-saturated T1-weighted images (Figure 10).

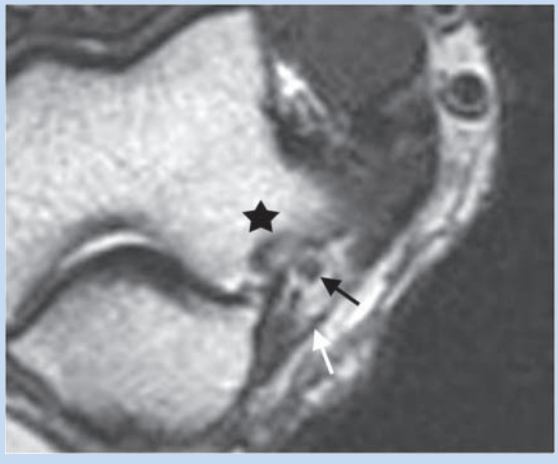

Figure 5. Normal anatomy of the ulnar nerve in the cubital tunnel. Axial proton density–weighted image demonstrates normal ulnar nerve (black arrow) in the cubital tunnel. The cubital tunnel is bordered by the medial epicondyle anteriorly (star) and the arcuate ligament posteriorly (white arrow).

Pearls:

- Look for fracture first.
- Use bone marrow edema as a clue of injury mechanism.
- Identify common patterns of injury.

Pitfalls:

- Pseudodefect of the capitellum.
- Stress fractures/stress reaction can be overlooked on T1-weighted images.
- OCD and loose bodies.

Muscles and Tendons

Evaluation of the elbow on MRI must include careful examination of the muscles and tendons of the 4 major muscle groups: medial, lateral, anterior, and posterior.

The proximal tendon of the medial group, the common flexor tendon, arises from the medial epicondyle and is best visualized in the coronal and axial planes. Like most tendons, it is usually uniformly low signal intensity on T1- and T2-weighted images.[27] Repetitive valgus stress involving the medial muscle group can lead to tendinopathy, partial tearing, or complete tearing of the common flexor tendon. This is visualized on MRI as changes in tendon diameter or increased signal on fat-saturated T2-weighted images within either the tendon or the adjacent medial epicondyle (medial epicondylitis or golfer's elbow; Figure 11).[2,10,18,23,27]

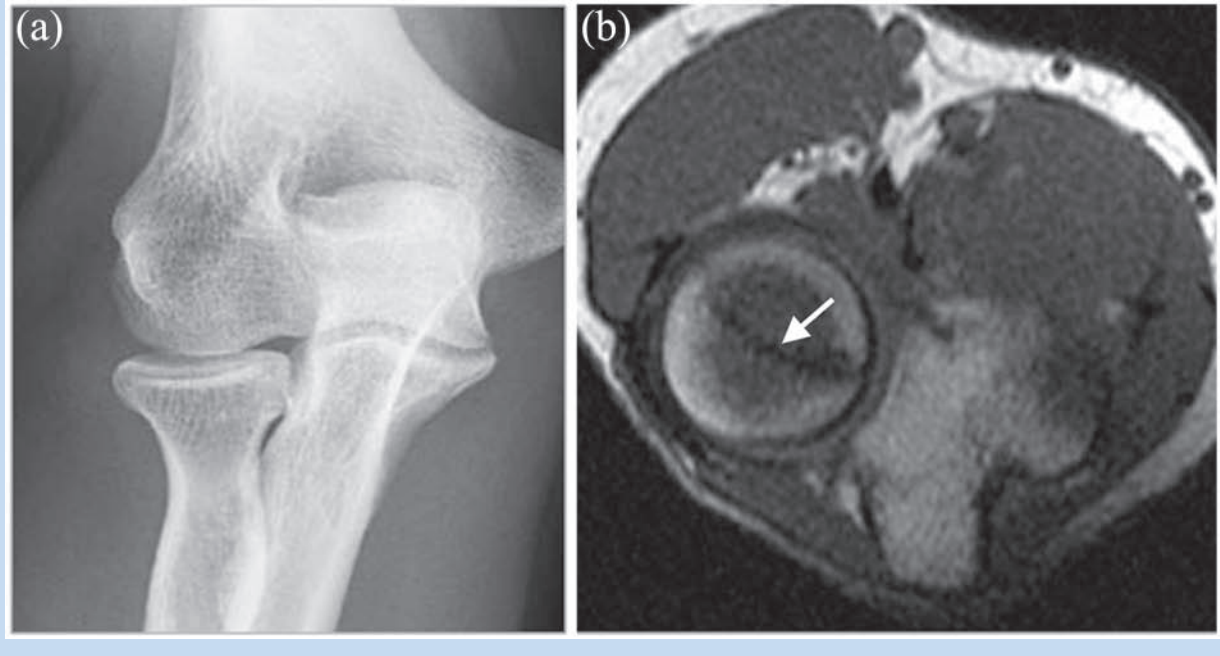

Figure 6. Radiographically occult radial head fracture. (a) Anteroposterior radiograph of the elbow in a patient who presented with elbow pain after a fall demonstrates no evidence of fracture. (b) Axial T1-weighted image demonstrates hypointense fracture line of the radial head (arrow).

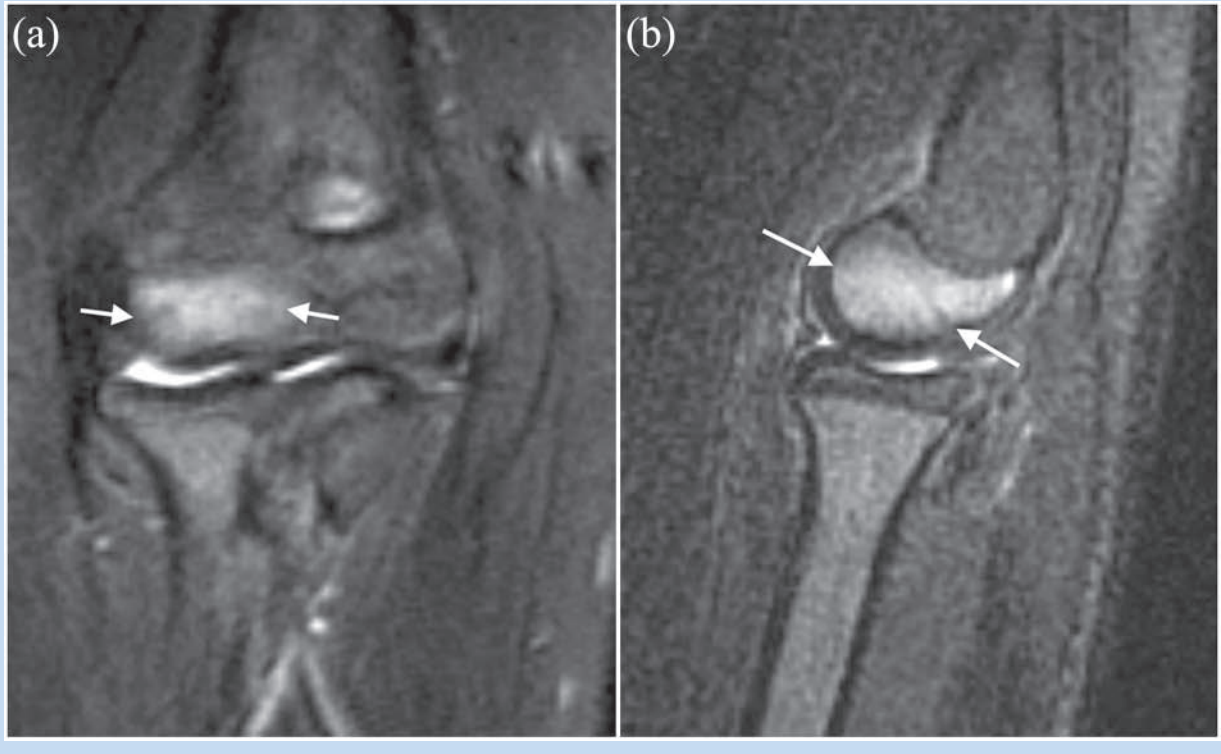

Figure 7. Coronal (a) and sagittal (b) fat-saturated T2-weighted images in a boy with Panner disease demonstrate bone marrow edema of the capitellar epiphysis (arrows). Bone marrow edema involves the entire capitellum with no discrete osteochondral defects identified.

Similarly, repetitive varus stress involving the proximal tendon of the lateral muscle group, the common extensor tendon, which arises from the lateral epicondyle of the humerus, can lead to tendinopathy or tearing (lateral epicondylitis, or tennis elbow; Figure 12), a condition many times more frequent than medial epicondylitis. The common extensor tendon is best evaluated in the coronal and axial planes, along with careful inspection of the lateral epicondyle on fat-saturated T2-weighted images.[2,10,16,18,23,25,27]

Injuries to the common flexor or extensor tendons frequently coincide with trauma to the adjacent ligaments. Associated injury to the LUCL occurs in the lateral epicondylitis (Figure 13).[3] Injury to any medial or lateral structure should prompt close examination of the adjacent soft tissues.

The main distal tendon of the anterior muscle group is the biceps tendon, which inserts onto the radial tuberosity and is involved in both flexion and supination of the forearm. The tendon is best evaluated in the axial and sagittal planes. Rupture of the distal biceps tendon is rare, representing < 5% of all biceps tendon injuries.[45] It is recognized by absence of the low signal tendon at the radial tuberosity insertion site or by a gap within the tendon and a variable degree of retraction of the proximal portion of the tendon (Figure 14). It might be necessary to increase the field of view to include the retracted tendon. Of note, the bicipital aponeurosis, or lacertus fibrosis (Figure 15), can act to restrict

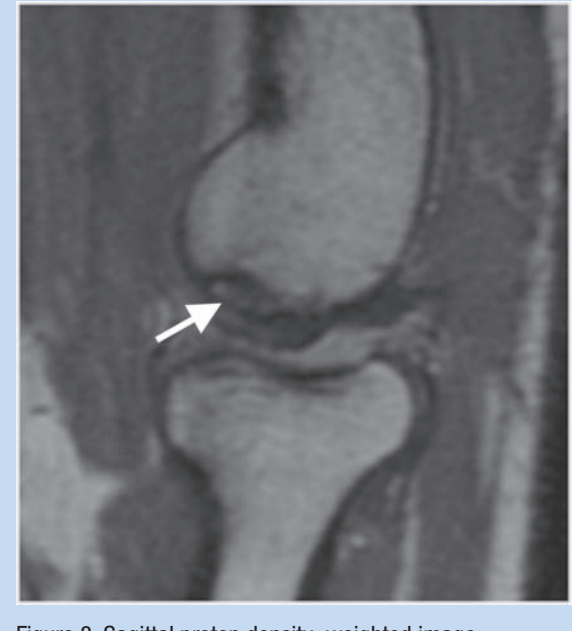

Figure 8. Sagittal proton density–weighted image demonstrates osteochondral lesion of the capitellum with irregularity of the articular surface (arrow).

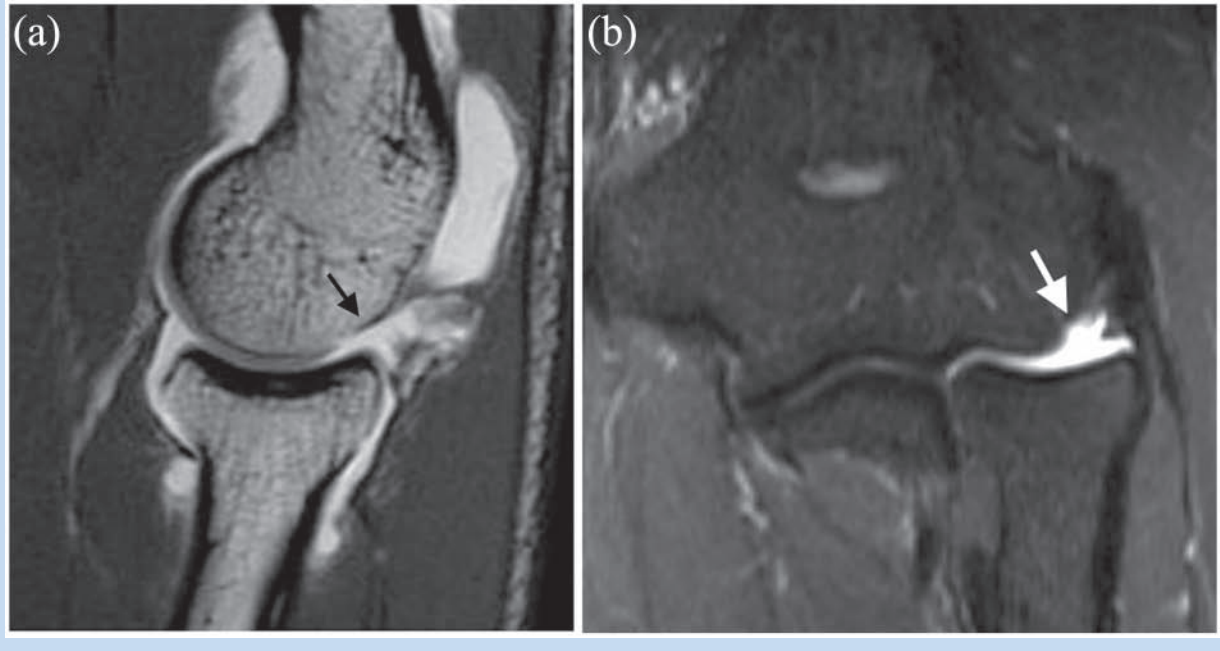

Figure 9. Pseudodefect of the capitellum. (a) Sagittal T1-weighted image from a magnetic resonance arthrogram demonstrates normal radiocapitellar articulation. Irregularity of the posterior capitellum (arrow) is devoid of cartilage and a nonarticulating area. (b) Pseudodefect of the capitellum (arrow) in the coronal plane on a fat-saturated T2-weighted image.

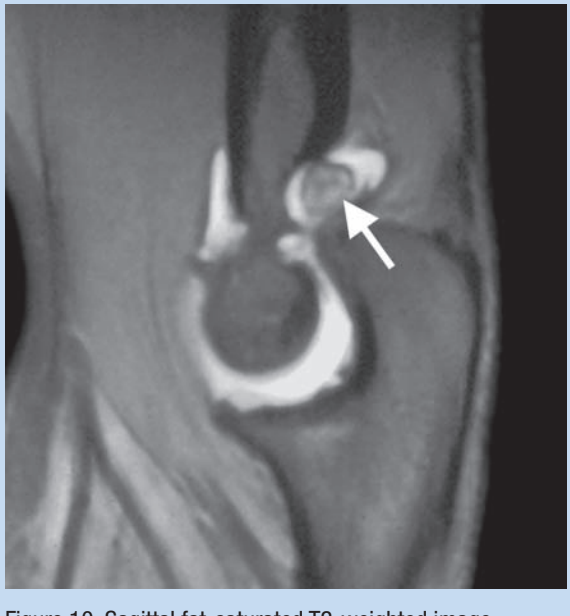

Figure 10. Sagittal fat-saturated T2-weighted image from a magnetic resonance arthrogram demonstrates a hypointense filling defect in the olecranon fossa, consistent with a loose body (arrow).

proximal retraction of a completely torn tendon; therefore, the degree of retraction is an imperfect indicator of complete versus partial tear. As with other tendinous injuries, partial tears of the distal biceps tendon can be evidenced by changes in tendon diameter, as well as possible increased intrasubstance signal on T2-weighted images.[13] Moreover, the distal biceps tendon is separated from the anterior aspect of the radial tuberosity by the bicipitoradial bursa, which is not usually visualized unless inflamed (Figure 16). Evaluation for bicipitoradial bursitis can therefore be a useful sign of partial tearing of the distal biceps tendon but should not be mistaken for a distal biceps tear.[5,13]

Injury to the main tendon of the posterior muscle group, the triceps tendon, is rare. The tendon is best evaluated in the axial or sagittal planes and usually tears at its insertion onto the olecranon process of the ulna, which can lead to an avulsion fracture.[12] Like the biceps tendon, both partial and complete tearing can occur, the latter with varying degrees of retraction. Evaluation is best performed on fat-saturated T2-weighted images, where tendon size, tendon signal intensity, and ulnar bone marrow signal intensity can be assessed (Figure 17).

Pearls:

- Assess tendon diameter/signal intensity on T1 and fat-saturated T2-weighted images.
- Look for injuries to the common flexor and extensor tendons in conjunction with injuries to the corresponding collateral ligaments.
- Partial tearing of the distal biceps tendon is often accompanied by bicipitoradial bursitis.
- Significant retraction of a complete biceps tendon tear may imply injury to the biceps aponeurosis (lacertus fibrosus).

Figure 11. Common flexor tendon injuries. (a) Coronal fat-saturated T2-weighted image demonstrates fluid signal within the common flexor tendon origin, consistent with partial tear (arrow). Coronal (b) and axial (c) fat-saturated T2-weighted images from a magnetic resonance arthrogram demonstrate full-thickness tear of the common flexor tendon from the medial epicondyle with tendon retraction and fluid signal in the expected location of the tendon (arrow).

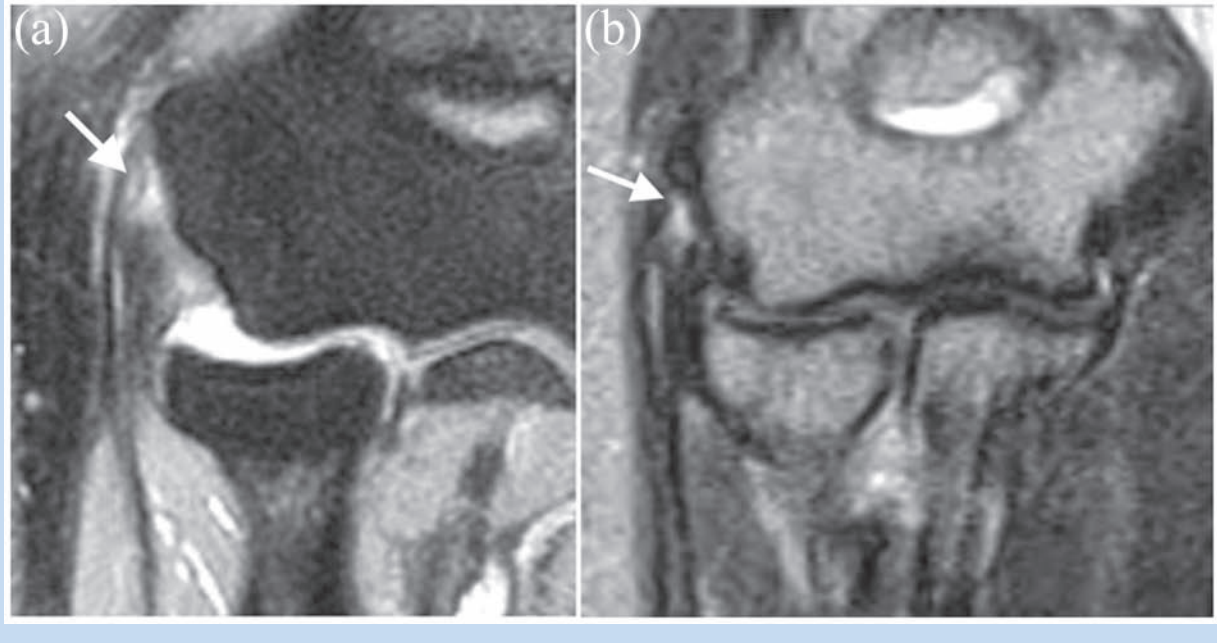

Figure 12. Common extensor tendon injury. (a) Coronal fat-saturated T2-weighted image demonstrates tendinopathy and partial tear of common extensor origin (arrow). (b) Coronal proton density–weighted image demonstrates partial tear of common extensor origin (arrow).

Pitfalls:

- Increased signal and thickness of the common flexor/extensor tendons may be present in asymptomatic athletes or after corticosteroid injection.
- Tendon injury may manifest as bone marrow signal change upon insertion, rather than in the tendon itself.

Ligaments

The ulnar (medial) collateral ligament is composed of anterior, posterior, and transverse bands, of which the anterior band is the most important stabilizer, followed by the posterior band. The ulnar collateral ligament acts mainly as a restraint to valgus stress at the elbow and is therefore most commonly

Figure 13. Coronal fat-saturated T1-weighted image from a magnetic resonance arthrogram demonstrates partial tear of common extensor origin and proximal lateral ulnar collateral ligament (arrow).

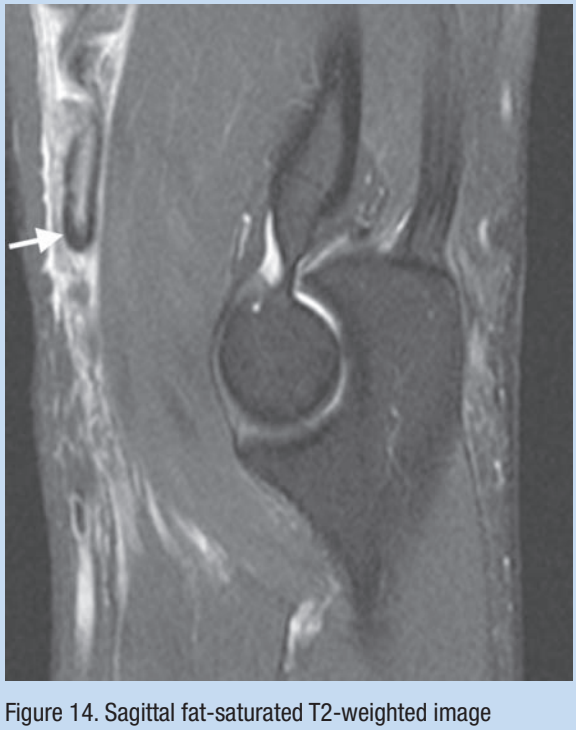

Figure 14. Sagittal fat-saturated T2-weighted image demonstrates biceps tendon rupture with tendon retraction. Note abnormal signal and thickening of retracted tendon (arrow). In some cases, it may be necessary to extend the field of view to include the retracted biceps tendon.

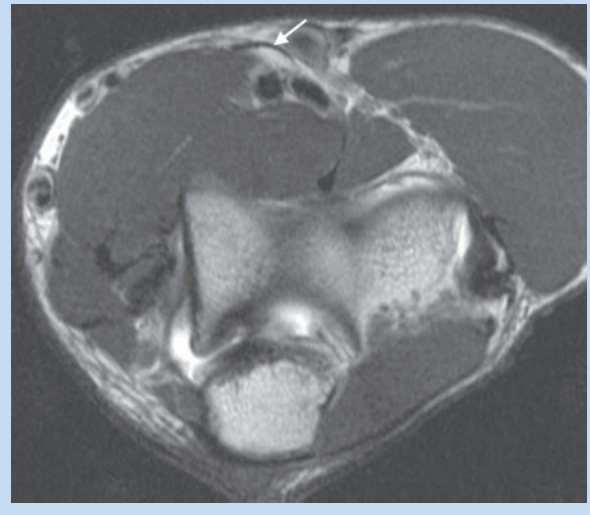

Figure 15. Axial proton density–weighted image shows normal appearance of the lacertus fibrosis (bicipital aponeurosis; arrow).

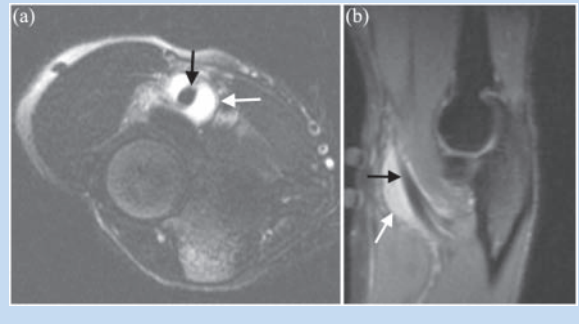

Figure 16. Bicipitoradial bursitis. Axial (a) and sagittal (b) fat-saturated T2-weighted images demonstrate fluid (white arrow) surrounding the distal biceps tendon (black arrow), consistent with bicipitoradial bursitis. This should not be mistaken for a distal biceps tear.

injured by activities requiring overhead throwing, such as pitching in baseball. Repetitive trauma results in microtears of the ligament, leading to weakening and, if untreated, rupture.[1,30,41]

On MRI, the anterior band is the most reliably identified component of the ulnar collateral ligament and extends from the medial epicondyle to the sublime tubercle at the medial base of the coronoid process of the ulna (see Figure 2). Ligament injuries can manifest as discontinuity (with T2 hyperintense fluid filling the gap), irregularity, or laxity (Figures 18a and 18b).[10] Midsubstance tears of the ulnar collateral ligament are more common; however, soft tissue or bony avulsion at either the proximal or distal attachment can occur (Figure 18c). Partial-thickness tears are particularly important to identify when they involve the deep articular fibers of the anterior bundle; these

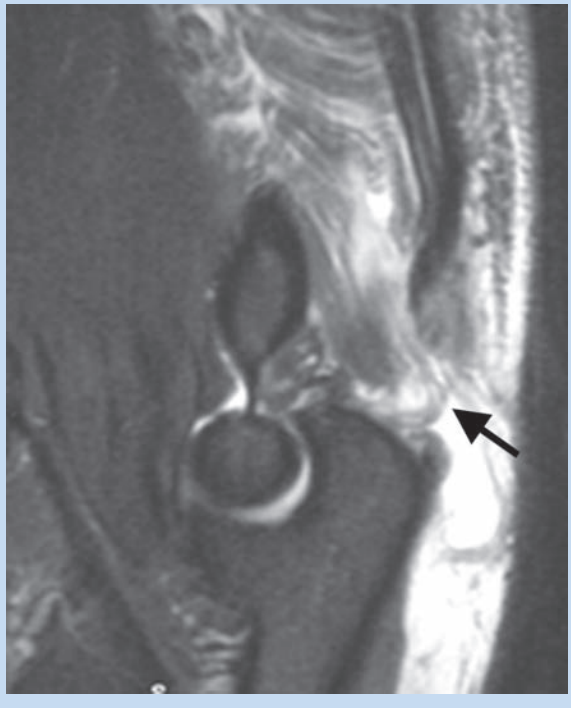

Figure 17. Sagittal fat-saturated T2-weighted image demonstrates triceps rupture with tendon retraction (arrow) and surrounding fluid/hemorrhage.

can be obscured at surgery by the overlying normal superficial fibers.[4] MRA may be helpful when partial-thickness tearing is suspected. Partial-thickness tears of the distal deep fibers of the anterior band of the ulnar collateral ligament near its insertion onto the sublime tubercle have been described on MRA as having a T-shaped appearance ("T sign"; Figure 19).[43] This should not be confused with a normal separation of the distal insertion of the anterior bundle of the ulnar collateral ligament and the sublime tubercle, which can be seen in approximately 50% of individuals.[32]

The radial (lateral) collateral ligament complex acts as the major counterpoint to varus stress. The complex consists of the radial collateral ligament, LUCL, annular ligament, and accessory collateral ligament (see Figure 3). Of these, the LUCL is the major varus stabilizer, and isolated tears of this ligament result in posterolateral rotatory instability.[33] This form of instability is distinct from recurrent dislocation of the elbow (radiohumeral or ulnohumeral) or radial head (radioulnar), all of which involve tearing of the annular ligament, whereas posterolateral rotatory instability does not. The LUCL is best seen as a hypointense structure on coronal T1-weighted images, extending from the lateral epicondyle across the elbow joint and posterior to the neck of the radius to insert on the supinator crest of the proximal ulna.[22] Given the complex course of the LUCL, it is often incompletely visualized on coronal images alone and is best evaluated in its entirety on multiplanar or 3-dimensional imaging sequences.

The most common injury to the LUCL is soft tissue avulsion at the proximal humeral attachment, often with concomitant injury to the common origin of the radial collateral ligament. Such injuries in adults are usually the result of varus stress without dislocation, whereas elbow dislocation more commonly accompanies this injury in younger individuals. As with the ulnar collateral ligament, partial tears of the LUCL and radial collateral ligament can be seen as areas of incomplete fluid signal within the ligament, in addition to thickening, thinning, or increased T2 signal. Injuries of the LUCL commonly accompany common extensor tendon or

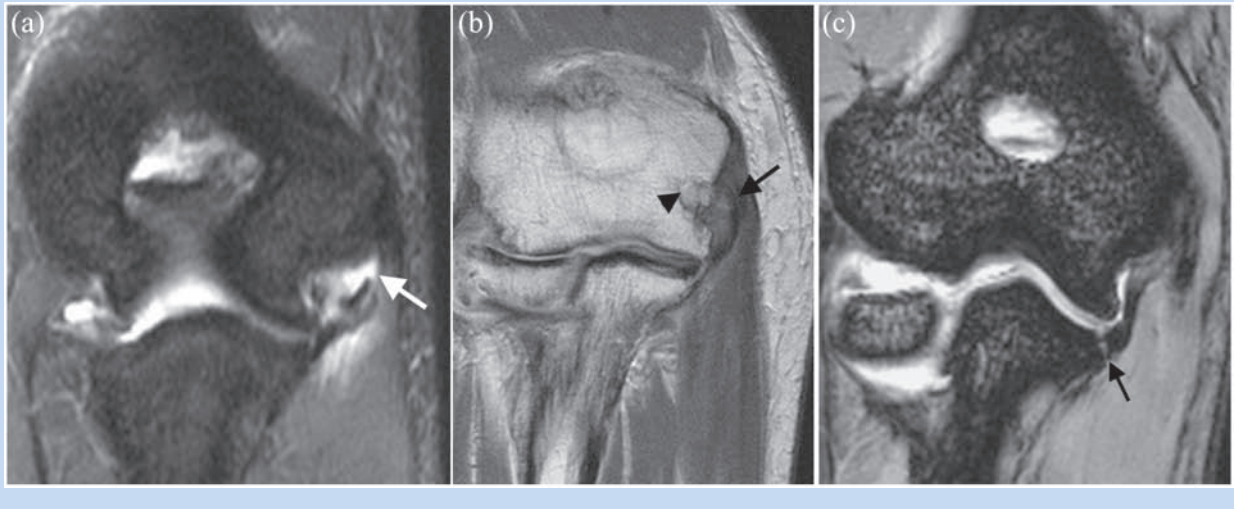

Figure 18. Ulnar collateral ligament injury. (a) Coronal fat-saturated T2-weighted image demonstrates complete tear of the ulnar collateral ligament, with fluid-filled gap between ligament fibers (arrow). (b) Coronal proton density–weighted image in a baseball pitcher demonstrates marked thickening with chronic tear of the ulnar collateral ligament (arrow). Note the associated osseous reactive change (arrowhead). (c) Coronal gradient echo image in a different baseball pitcher demonstrates avulsion of the sublime tubercle (arrow).

Figure 19. "T sign" of ulnar collateral ligament partial tear. Coronal fat-saturated T1-weighted image from a magnetic resonance arthrogram demonstrates contrast extending along the medial aspect of the sublime tubercle with disruption of the distal fibers of the ulnar collateral ligament (arrow).

Figure 20. Coronal fat-saturated T2-weighted image demonstrates tendinopathy and tear of the common extensor tendon (white arrow) as well as tear of the proximal lateral ulnar collateral ligament (black arrow). Note associated bone marrow edema of the lateral epicondyle (star).

lateral epicondyle abnormalities (Figure 20), and these should be carefully evaluated if the LUCL is abnormal.[3]

The other lateral stabilizer of the elbow, the annular ligament, is a thick structure encircling the radial head and inserting on the anterior and posterior aspects of the sigmoid notch of the ulna. It is less commonly injured than the LUCL but demonstrates similar signal changes when affected. It should be carefully scrutinized in suspected dislocation; it must be injured to allow independent movement or dislocation of either the radial head or the olecranon.

Pearls:

- The ulnar collateral ligament is the primary medial elbow stabilizer and the LUCL, the primary lateral—look for them!
- MRA may enhance detection of partial-thickness ligament tears.
- Dislocation at the elbow usually implies annular ligament tear.
- Look for tendon or bone injury in cases of ligamentous injury (and vice versa).

Pitfalls:

- Partial-thickness ligament tears can be occult at surgery, despite markedly limiting function.
- The LUCL may be incompletely visualized on coronal images alone.

Valgus Extension Overload Syndrome

The elbow is frequently injured in overhead throwing athletes, especially in baseball pitchers, due to repetitive excessive valgus forces during the throwing cycle. Typical injuries are secondary to medial joint distraction, lateral joint compression, and rotatory forces at the olecranon (Figure 21). MRI is the modality of choice in evaluating elbow injuries in throwing athletes.[34,35]

During the throwing cycle, high valgus stress is applied to the elbow, giving rise to high distraction stress at the medial compartment. This causes injuries to the medial elbow soft tissue restraints—namely, the ulnar collateral ligament and common flexor tendon. The valgus stress also causes compressive forces to the lateral compartment, which can lead to osteochondral defects of the capitellum. In addition, valgus forces during rapid elbow extension can lead to shear forces to the posteromedial olecranon, which can cause osteophyte formation of the posteromedial olecranon (Figure 22).[4,34,35,47]

Nerves

The 3 major nerves of the elbow are the ulnar, radial, and median nerves. These are derived from the roots of C5-T1 and give motor and sensory supply to the forearm and hand. Normal nerves demonstrate a signal that is isointense to muscle on T1 and isointense to slightly hyperintense to muscle on T2 or proton density–weighted images. The nerves are best visualized when surrounded by fat. Abnormal nerves can have

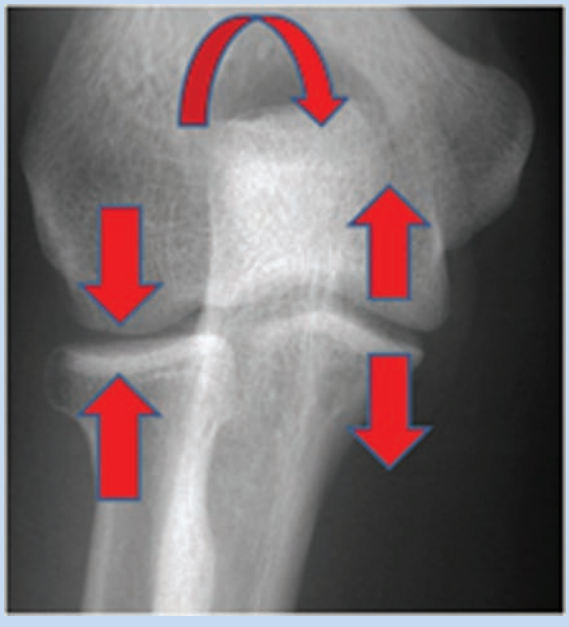

Figure 21. Valgus extension overload syndrome. Anteroposterior radiograph demonstrates the mechanism of valgus extension overload syndrome. Injuries occur secondary to medial joint distraction, lateral joint compression, and posterior rotatory shear forces.

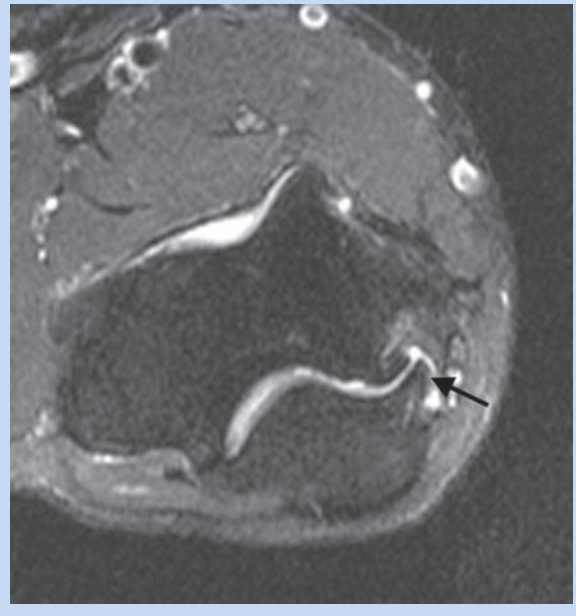

Figure 22. Axial fat-saturated T2-weighted image in a baseball pitcher with valgus extension overload syndrome demonstrates prominent posterior osteophyte at the medial olecranon (arrow).

a variety of appearances at MRI, including focal or diffuse enlargement, high T2 signal, and swelling or indistinctness of the fascicles of which the nerve is composed.[38] In severe cases, the nerve can have a nearly cystic appearance. These changes are in general best imaged in the axial plane, although the coronal and sagittal planes can also be useful.

Of the nerves of the elbow, the ulnar nerve is the largest, most easily imaged, most superficial, and most commonly injured and is therefore evaluated first. The ulnar nerve is readily identified as is passes through the superficial cubital tunnel (see Figure 5), completely surrounded by fat. Given its superficial location, the ulnar nerve is most susceptible to trauma as well as impingement from degenerative changes or other causes. Any process that impinges on the nerve at this level may cause ulnar impingement (cubital tunnel syndrome) and result in ulnar neuropathy (Figure 23). While the ulnar nerve can be also injured or compressed above and below the elbow, impingement within the cubital tunnel is the most common cause of ulnar neuropathy.[29,39]

The floor of the cubital tunnel contains the posterior and transverse bands of the ulnar collateral ligament, which can compress the ulnar nerve when torn or degenerated. The roof of the cubital tunnel is formed proximally by the cubital tunnel retinaculum (arcuate ligament) and distally by the deep fibers of the flexor carpi ulnaris aponeurosis. In approximately 10% to 20% of individuals, the retinaculum is replaced by an accessory muscle, the anconeus epitrochlearis (see Figure 4f), which may cause static or dynamic compression of the ulnar nerve within the tunnel.[19] Similar compression can be caused by direct trauma or posttraumatic bony deformity, ganglia, bursae, and degenerative osteophytic change of the elbow. Ulnar neuritis is also a common symptom in throwing athletes, as the cubital tunnel narrows during elbow flexion. Over 40% of throwing athletes with medial instability of the elbow have ulnar neuritis, and over 60% of overhead throwing athletes with medial epicondylitis experience ulnar nerve symptoms.[6,15]

In comparison with the ulnar nerve, the radial nerve is much less commonly injured. Traumatic injury is most common above the level of the elbow, often due to displaced fractures of the humerus. The radial nerve divides at the elbow into a superficial sensory branch and a deep motor branch, the posterior interosseous nerve. The posterior interosseous nerve can be impinged at any level in the so-called radial tunnel, which extends from the level of the lateral epicondyle to the proximal forearm at the level of the supinator muscle (Figure 24). Radial nerve impingement is often seen as an overuse injury and, when proximal, can mimic or exacerbate lateral epicondylitis. A classic form of more distal impingement is supinator syndrome, which is caused by compression of the posterior interosseous nerve as it courses beneath the arcade of Frohse, a fibrous band associated with the superficial head of the supinator muscle.[20] This can present clinically as pure motor weakness of the abductor pollicis longus and extensor muscle groups.

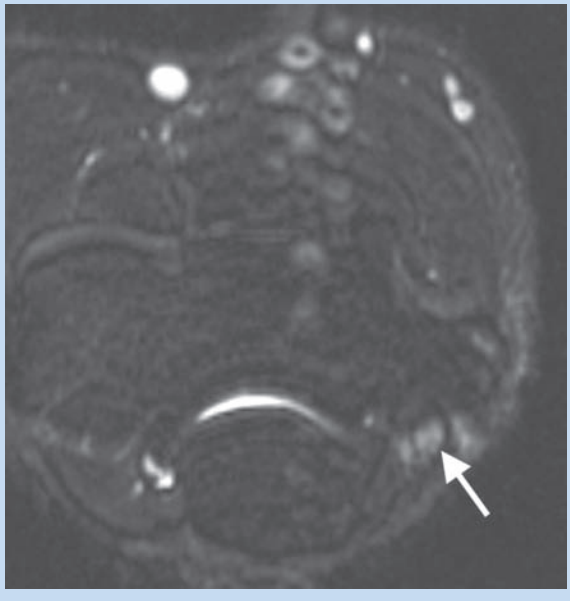

Figure 23. Axial fat-saturated T2-weighted image demonstrates enlargement and increased signal of the ulnar nerve in the cubital tunnel (arrow), consistent with ulnar neuritis.

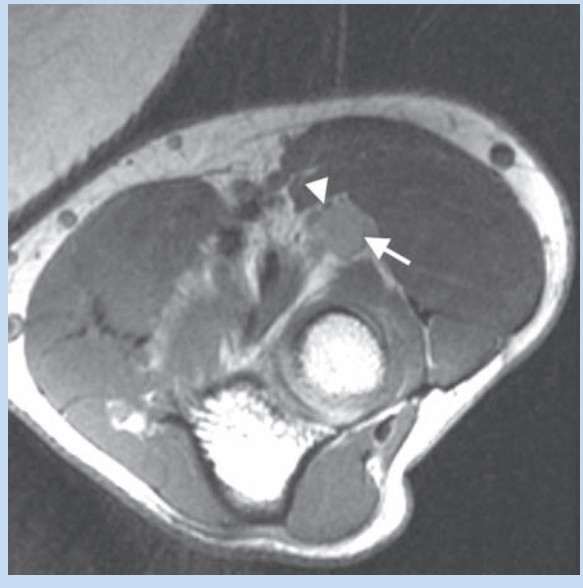

Figure 24. Axial proton density–weighted image demonstrates a ganglion (arrow) adjacent to the posterior interosseous nerve (arrowhead).

Pearls:

- Carefully scrutinize the cubital tunnel, assessing for an anconeus epitrochlearis and for bony impingement from osteophytes.
- Look for associated denervation changes in muscles to guide assessment of the related nerves.

Pitfalls:

- Distinguish radial nerve compression from lateral epicondylitis.
- Be aware of the limitations imposed by standard imaging position.

Synovium and Bursae

MRI evaluation of the elbow would be incomplete without consideration of the synovium and bursae. As with synovial joints elsewhere in the body, synovitis of the elbow can occur as a result of infectious, inflammatory, or posttraumatic conditions. The appearance is nonspecific on MRI but generally includes a T2-hyperintense joint effusion, synovial hypertrophy, and prominent enhancement if intravenous gadolinium is administered. In subjects with rheumatoid arthritis, bony erosions and T2-hyperintense pannus may also be seen. The joint fluid in uncomplicated effusion is generally T1 hypointense but may become isointense or complex if there is significant synovitis or superinfection.[21,44] Specific sequences, such as gradient echo imaging, may add specificity to the evaluation of synovial processes. For instance, both hemophiliac arthropathy and pigmented villonodular synovitis will show "blooming," or pronounced signal dropout, on gradient echo sequences due to the dephasing effects of iron/hemosiderin (Figure 25).[28,36]

Finally, examination should be made for abnormal fluid/bursal collections. The most common bursae include the bicipitoradial bursa (discussed previously; see Figure 16) and olecranon bursa.[14] The latter lies superficial to the olecranon process and is abnormal if visible (Figure 26). Common etiologies include infection and gout, which, as elsewhere, appear as intermediate in T1 signal with significant variability on T2-weighted images.

Pearls:

- Look for signs that provide specificity to the cause of synovitis (eg, osseous erosion).
- Consider additional sequences (eg, gradient echo) if a synovial process is suspected.

Pifalls:

- Always consider infection!

CONCLUSION

A systematic approach to MRI evaluation of the elbow will allow quick identification of most abnormalities. Evaluation should include bones; lateral, medial, anterior, and posterior muscle groups; the ulnar and radial collateral ligaments; as well as nerves, synovium, and bursae. Special attention should be paid to the valgus extension overload syndrome and the MRI appearance of associated injuries when evaluating

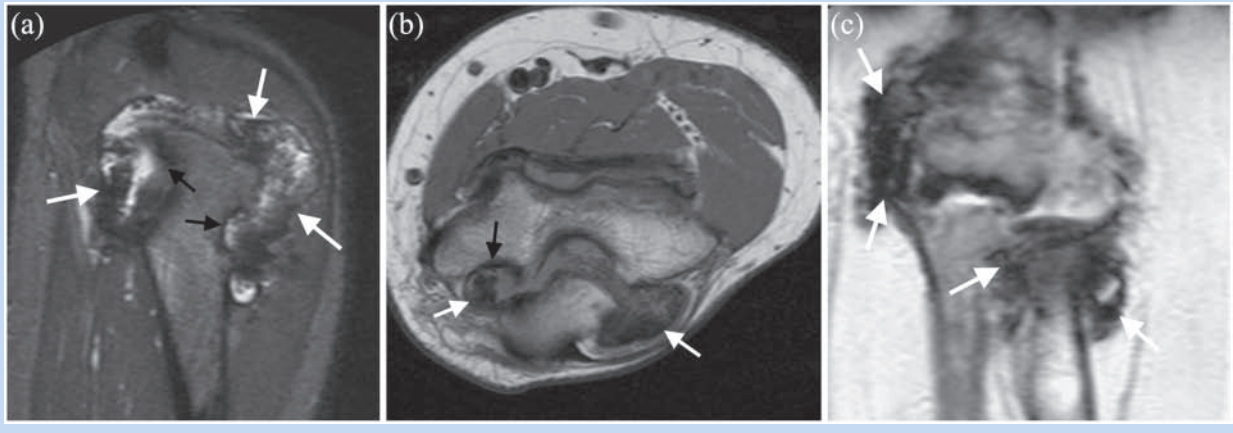

Figure 25. Hemophilia in a 20-year-old man. Posterior coronal fat-saturated T2-weighted (a) and axial proton density–weighted (b) images demonstrate extensive synovial proliferation (white arrows), predominately low signal intensity, consistent with blood products. Note associated large erosions (black arrows). (c) Coronal localizer gradient echo image demonstrates "blooming" artifact from hemosiderin (white arrows).

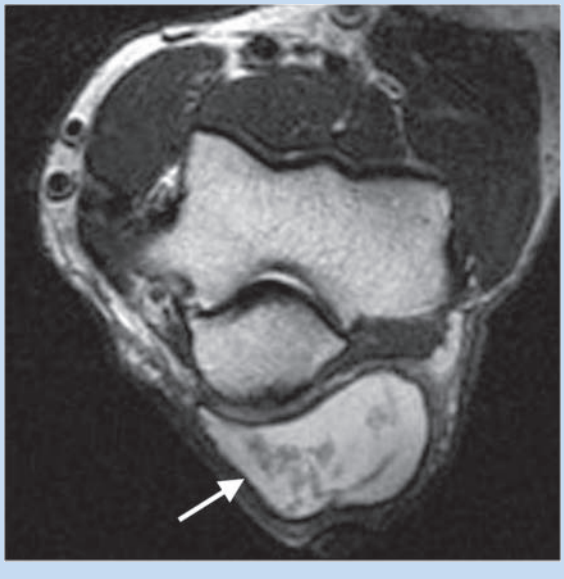

Figure 26. Axial T2-weighted image demonstrates marked enlargement of the olecranon bursa (arrow) with internal debris, consistent with olecranon bursitis.

throwing athletes. It is hoped that the current brief discussion will provide a foundation for further understanding of this complex and commonly injured joint.

REFERENCES

1. Alcid JG, Ahmad CS, Lee TQ. Elbow anatomy and structural biomechanics. *Clin Sports Med.* 2004;23(4):503-517.
2. Biundo JJ Jr, Mipro RC Jr, Fahey P. Sports-related and other soft-tissue injuries, tendinitis, bursitis, and occupation-related syndromes. *Curr Opinion in Rheumatol.* 1997;9(2):151-154.
3. Bredella MA, Tirman PF, Fritz RC, et al. MR imaging findings of lateral ulnar collateral ligament abnormalities in patients with lateral epicondylitis. *AJR Am J Roentgenol.* 1999;173(5):1379-1382.
4. Cain EL Jr, Dugas JR, Wolf RS, et al. Elbow injuries in throwing athletes: a current concepts review. *Am J Sports Med.* 2003;31(4):621-635.
5. Chew ML, Giuffre BM. Disorders of the distal biceps brachii tendon. *Radiographics.* 2005;25(5):1227-1237.
6. Conway JE, Jobe FW, Glousman RE, et al. Medial instability of the elbow in throwing athletes: treatment by repair or reconstruction of the ulnar collateral ligament. *J Bone Joint Surg Am.* 1992;74(1):67-83.
7. Cunningham PM. MR imaging of trauma: elbow and wrist. *Semin Musculoskelet Radiol.* 2006;10(4):284-292.
8. De Smet AA, Winter TC, Best TM, et al. Dynamic sonography with valgus stress to assess elbow ulnar collateral ligament injury in baseball pitchers. *Skeletal Radiol.* 2002;31(11):671-676.
9. Delport AG, Zoga AC. MR and CT arthrography of the elbow. *Semin Musculoskelet Radiol.* 2012;16(1):15-26.
10. Desharnais L, Kaplan PA, Dussault RG. MR imaging of ligamentous abnormalities of the elbow. *Magn Reson Imaging Clin N Am.* 1997;5(3):515-528.
11. Emery KH. MR imaging in congenital and acquired disorders of the pediatric upper extremity. *Magn Reson Imaging Clin N Am.* Aug 2009;17(3):549-570.
12. Farrar EL 3rd, Lippert FG 3rd. Avulsion of the triceps tendon. *Clin Orthop Relat Res.* 1981;161:242-246.
13. Fitzgerald SW, Curry DR, Erickson SJ, et al. Distal biceps tendon injury: MR imaging diagnosis. *Radiology.* 1994;191(1):203-206.
14. Floemer F, Morrison WB, Bongartz G, et al. MRI characteristics of olecranon bursitis. *AJR Am J Roentgenol.* 2004;183(1):29-34.
15. Gabel GT, Morrey BF. Operative treatment of medical epicondylitis: influence of concomitant ulnar neuropathy at the elbow. *J Bone Joint Surg Am.* 1995;77(7):1065-1069.
16. Gabel GT, Morrey BF. Tennis elbow. *Instructional Course Lectures.* 1998;47:165-172.
17. Herzog RJ. Magnetic resonance imaging of the elbow. *Magn Reson Q.* 1993;9(3):188-210.
18. Ho CP. MR imaging of tendon injuries in the elbow. *Magn Reson Imaging Clin N Am.* 1997;5(3):529-543.
19. Husarik DB, Saupe N, Pfirrmann CW, et al. Elbow nerves: MR findings in 60 asymptomatic subjects—normal anatomy, variants, and pitfalls. *Radiology.* 2009;252(1):148-156.
20. Jacobson JA, Fessell DP, Lobo Lda G, et al. Entrapment neuropathies: I. Upper limb (carpal tunnel excluded). *Semin Musculoskelet Radiol.* 2010;14(5):473-486.
21. Jbara M, Patnana M, Kazmi F, et al. MR imaging: arthropathies and infectious conditions of the elbow, wrist, and hand. *Radiol Clin North Am.* 2006;44(4):625-642.

22. Kijowski R, Tuite M, Sanford M. Magnetic resonance imaging of the elbow: part I. Normal anatomy, imaging technique, and osseous abnormalities. *Skeletal Radiol.* 2004;33(12):685-697.
23. Kijowski R, Tuite M, Sanford M. Magnetic resonance imaging of the elbow: part II. Abnormalities of the ligaments, tendons, and nerves. *Skeletal Radiol.* 2005;34(1):1-18.
24. Kobayashi K, Burton KJ, Rodner C, et al. Lateral compression injuries in the pediatric elbow: Panner's disease and osteochondritis dissecans of the capitellum. *J Am Acad Orthop Surg.* 2004;12(4):246-254.
25. Kotnis NA, Chiavaras MM, Harish S. Lateral epicondylitis and beyond: imaging of lateral elbow pain with clinical-radiologic correlation. *Skeletal Radiol.* 2012;41(4):369-386.
26. Mallisee TA, Boynton MD, Erickson SJ, et al. Normal MR imaging anatomy of the elbow. *Magn Reson Imaging Clin N Am.* 1997;5(3): 451-479.
27. Martin CE, Schweitzer ME. MR imaging of epicondylitis. *Skeletal Radiol.* 1998;27(3):133-138.
28. Masih S, Antebi A. Imaging of pigmented villonodular synovitis. *Semin Musculoskelet Radiol.* 2003;7(3):205-216.
29. Miller RG. The cubital tunnel syndrome: diagnosis and precise localization. *Ann Neurol.* 1979;6(1):56-59.
30. Morrey BF, An KN. Functional anatomy of the ligaments of the elbow. *Clin Orthop Relat Res.* 1985;201:84-90.
31. Morrey BF, An KN. Stability of the elbow: osseous constraints. *J Shoulder Elbow Surg.* 2005;14(1)(suppl S):174S-178S.
32. Munshi M, Pretterklieber ML, Chung CB, et al. Anterior bundle of ulnar collateral ligament: evaluation of anatomic relationships by using MR imaging, MR arthrography, and gross anatomic and histologic analysis. *Radiology.* 2004;231(3):797-803.
33. O'Driscoll SW, Bell DF, Morrey BF. Posterolateral rotatory instability of the elbow. *J Bone Joint Surg Am.* 1991;73(3):440-446.
34. Ouellette H, Bredella M, Labis J, et al. MR imaging of the elbow in baseball pitchers. *Skeletal Radiol.* 2008;37(2):115-121.
35. Ouellette HA, Palmer W, Torriani M, et al. Throwing elbow in adults. *Semin Musculoskelet Radiol.* 2010;14(4):412-418.
36. Rand T, Trattnig S, Male C, et al. Magnetic resonance imaging in hemophilic children: value of gradient echo and contrast-enhanced imaging. *Magn Reson Imaging.* 1999;17(2):199-205.
37. Rosenberg ZS, Beltran J, Cheung YY. Pseudodefect of the capitellum: potential MR imaging pitfall. *Radiology.* 1994;191(3):821-823.
38. Rosenberg ZS, Beltran J, Cheung YY, et al. The elbow: MR features of nerve disorders. *Radiology.* 1993;188(1):235-240.
39. Rosenberg ZS, Bencardino J, Beltran J. MR features of nerve disorders at the elbow. *Magn Reson Imaging Clin N Am.* 1997;5(3):545-565.
40. Ruchelsman DE, Hall MP, Youm T. Osteochondritis dissecans of the capitellum: current concepts. *J Am Acad Orthop Surg.* 2010;18(9):557-567.
41. Safran MR, Baillargeon D. Soft-tissue stabilizers of the elbow. *J Shoulder Elbow Surg.* 2005;14(1)(suppl S):179S-185S.
42. Sampaio ML, Schweitzer ME. Elbow magnetic resonance imaging variants and pitfalls. *Magn Reson Imaging Clin N Am.* 2010;18(4):633-642.
43. Schwartz ML, al-Zahrani S, Morwessel RM, et al. Ulnar collateral ligament injury in the throwing athlete: evaluation with saline-enhanced MR arthrography. *Radiology.* 1995;197(1):297-299.
44. Schweitzer M, Morrison WB. Arthropathies and inflammatory conditions of the elbow. *Magn Reson Imaging Clin N Am.* 1997;5(3):603-617.
45. Seiler JG 3rd, Parker LM, Chamberland PD, et al. The distal biceps tendon: two potential mechanisms involved in its rupture: arterial supply and mechanical impingement. *J Shoulder Elbow Surg.* 1995;4(3):149-156.
46. Steinbach LS, Schwartz M. Elbow arthrography. *Radiol Clin North Am.* 1998;36(4):635-649.
47. Wilson FD, Andrews JR, Blackburn TA, et al. Valgus extension overload in the pitching elbow. *Am J Sports Med.* 1983;11(2):83-88.